



1 Estimation of land-use change using a 2 Bayesian data assimilation approach

3 *Peter Levy, Marcel van Oijen, Gwen Buys, and Sam Tomlinson*

4 *Centre for Ecology & Hydrology*

6 **Abstract**

7 We present a method for estimating land-use change using a Bayesian data assimilation
8 approach. The approach provides a general framework for combining multiple disparate data
9 sources with a simple model. This allows us to constrain estimates of gross land-use change
10 with reliable national-scale census data, whilst retaining the detailed information available
11 from several other sources. Eight different data sources, with three different data structures,
12 were combined in our posterior estimate of land-use and land-use change, and other data
13 sources could easily be added in future. The tendency for observations to underestimate
14 gross land-use change is accounted for by allowing for a skewed distribution in the likelihood
15 function. The data structure produced has high temporal and spatial resolution, and is
16 appropriate for dynamic process-based modelling. Uncertainty is propagated appropriately
17 into the output, so we have a full posterior distribution of output and parameters. The
18 data are available in the widely used netCDF file format from <http://eidc.ceh.ac.uk/> (doi
19 pending).

20



21 Introduction

22 Human-induced land-use change has a substantial impact on biodiversity and both biogeo-
23 chemical and hydrological cycles (Post & Kwon, 2000; Gitz & Ciais, 2003; Levy *et al.*, 2004;
24 Newbold *et al.*, 2015; Piano *et al.*, 2017). The importance of representing it in models of the
25 climate, hydrology, and ecosystem processes is increasingly recognised (Martin *et al.*, 2017;
26 Prestele *et al.*, 2017; Quesada *et al.*, 2017). However, although changes in land use tend to
27 occur incrementally over small areas, data on land-use change are typically limited in spatial
28 and temporal resolution (Alexander *et al.*, 2017). Furthermore, changes in land use may be
29 rotational or involve transitions between multiple land-use classes over time, such that the
30 gross area undergoing land-use change may be much larger than the net change in area (Fuchs
31 *et al.*, 2015; Tomlinson *et al.*, 2017). From the point of view of modelling ecosystem processes,
32 it is these fine-scale gross changes that we need to represent, because as model inputs, these
33 may give very different simulated output, compared with simulations based on the net change
34 at a coarse scale (Kato *et al.*, 2013; Wilkenskjeld *et al.*, 2014; Fuchs *et al.*, 2015). For example,
35 a reported net increase in forest area of 10 km² may actually result from afforestation of 50
36 km² and deforestation of 40 km². As input data to an ecosystem model, this might produce
37 quite different results, compared to the parsimonious assumption (afforestation of 10 km²
38 and no deforestation)(Levy & Milne, 2004; Krause *et al.*, 2016). Over most of the globe, data
39 on land-use change are typically limited in spatial and temporal resolution, and are typically
40 represented by a time series of the area occupied by each land-use class (Rounsevell *et al.*,
41 2006). Little information is available on the gross changes which bring about this time series
42 (Prestele *et al.*, 2017). The IPCC Good Practice Guidelines recommends the estimation of
43 land-use change matrices for reporting GHG fluxes arising from land-use change (Penman *et*
44 *al.*, 2003). This provides explicit information on the areas which have changed from each
45 land-use class to every other class. Whilst these matrices contain more information, they are
46 only valid over the single time period for which they were derived, being a two-dimensional



47 summary. For modelling over longer time periods, these are not very useful in themselves.
48 To properly represent the change in land use over time, we need a higher-dimensional data
49 structure.

50 Land-use change is not easy to measure. A key problem is identifying change from repeated
51 map or survey data, where the magnitude of the change signal is very small against the
52 background noise of sampling and measurement error. Large censuses and careful survey
53 techniques are required to distinguish true change from differences arising from measurement
54 and sampling error (Fuller *et al.*, 2003). A further problem is that information on land-use
55 change at national scale typically comes from multiple disparate sources, which are often
56 inconsistent with each other, using different land-use classifications and definitions (Phelps
57 & Kaplan, 2017), arising from different thematic areas, and focus on different spatial and
58 temporal domains, with different resolutions (Fisher *et al.*, 2017). For example, land-use data
59 in the UK are available from the agricultural census and surveys, the national forestry sector,
60 the national mapping survey, as well as earth observation products such as Corine, MODIS
61 and the CEH Land Cover Maps. However, no single data source provides a reliable estimate
62 of land-use change with national coverage which extends suitably far back in time. A data
63 assimilation approach is needed to make best use of the available data, so as to provide such
64 a product. Existing methods ignore the large uncertainties which arise in estimating past
65 land use change, and data assimilation approaches can explicitly address this issue.

66 In general terms, data assimilation is an approach for fusing observations with prior knowledge
67 (e.g., mathematical representations of physical laws; model output) to obtain an estimate of
68 the distribution of the true state of some phenomenon. It has become very commonly used
69 in fields such as atmospheric and oceanographic modelling, and numerical weather prediction
70 (e.g. Lunt *et al.*, 2016). Various techniques are used, such as simulated annealing, ensemble
71 Kalman filtering, and 4D variational assimilation. All of these can be seen as special cases
72 within the Bayesian framework, where models, parameters and data are related in a formal



73 way via Bayes Theorem (Wikle & Berliner, 2007). There are some significant differences in
74 applying data assimilation in our land-use context, compared with atmospheric modelling.
75 Firstly, there is only a very simple model, compared with the complex physical models of the
76 atmosphere or ocean. By contrast, the observational process by which the data are produced
77 is extremely complex, compared with the simple observations of air or sea temperature or
78 pressure. Also, we are predicting retrospectively (i.e. “hind-casting”) over many years in the
79 past, rather than “nudging” forecasts as new data becomes available.

80 Our aim here was to develop a generic Bayesian approach, using multiple sources of data, to
81 make spatially- and temporally-explicit estimates of land-use change. In a case study, we
82 apply the approach to Scotland over the period 1969-2015. As an example application, we
83 use a simple model of carbon fluxes following land-use change to show how uncertainties
84 surrounding land-use change can be propagated through to model output.

85 **Materials and methods**

86 **Mathematical approach and notation**

87 We represent land use u as a number of discrete states from the set {forest, crop, grassland, roughgrazing, urba
88 encoded as integers 1-6. At a single location (x,y) , land use can change between these states
89 over time, represented by the vector \mathbf{U}_{xy} . (We use a convention of representing vectors,
90 matrices and arrays as uppercase bold (e.g. \mathbf{U}), and individual elements thereof as uppercase
91 italic (e.g. U_{xyt} .) An example for $t = (1 \dots 5)$ would be $\mathbf{U}_{xy} = (4, 3, 3, 2, 2)$, showing a
92 change in land use from rough grazing (class 4) to grassland (class 3) for two years, then to
93 cropland (class 2) for two years. Spatially, we represent land use on a grid, where each grid
94 cell contains a vector of land use. Combining the spatial and temporal dimensions, we have
95 the 3-D space-time array $\mathbf{U} = \{U_{xyt}\}$ (Figure 1). This is the basic data structure required by
96 any model which models the effects of land use dynamically and spatially explicitly. Our aim



97 is to estimate the 3-D array \mathbf{U} as accurately as possible by constraining with multiple data
 98 sources. (We note that for the purposes of non-spatial modelling, there is a lot of redundancy
 99 in this data structure, and the information in \mathbf{U} can be condensed into the set of unique
 100 land-use vectors and their corresponding areas. We return to this point later.)

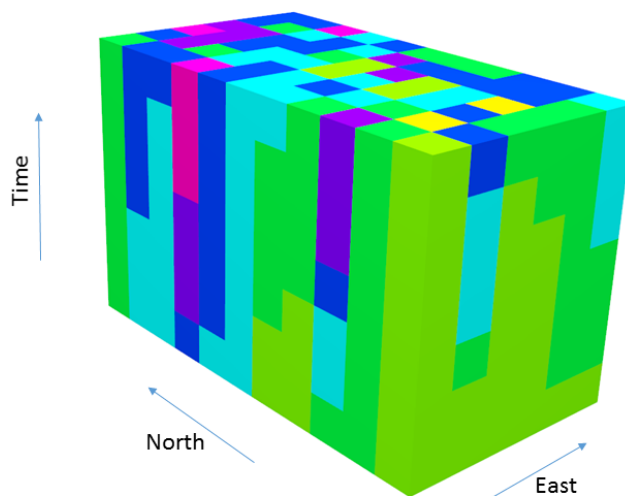


Figure 1: Graphical depiction of a hypothetical 3-D cuboid \mathbf{U} representing land use in space and time dimensions. Different colours show different land uses.

101 We denote the area occupied by each land use u at time t as A_{ut} , obtained by counting the
 102 frequency of land uses in \mathbf{U}_t :

$$A_{ut} = \sum_{x=1}^{n_x} \sum_{y=1}^{n_y} [U_{xyt} = u] A_{\text{gridcell}} \quad (1)$$

103 where the square brackets are Iverson notation, evaluating to 1 where true and zero otherwise,
 104 and A_{gridcell} is the area of a single grid cell. We denote the array of all these areas (for each



105 land-use class and time step) as $\mathbf{A} = \{A_{ut}\}$. By differencing, we obtain the areas of net
 106 land-use change:

$$\Delta A_{ut} = A_{ut} - A_{ut-1}. \quad (2)$$

107 At each time step, we have a square transition matrix

$$\mathbf{B} = \begin{bmatrix} 0 & \beta_{12} & \beta_{13} & \dots & \beta_{1n} \\ \beta_{21} & 0 & \beta_{23} & \dots & \beta_{2n} \\ \vdots & \vdots & \vdots & \ddots & \vdots \\ \beta_{n1} & \beta_{n2} & \beta_{n3} & \dots & 0 \end{bmatrix}_{t=1} \begin{bmatrix} 0 & \beta_{12} & \beta_{13} & \dots & \beta_{1n} \\ \beta_{21} & 0 & \beta_{23} & \dots & \beta_{2n} \\ \vdots & \vdots & \vdots & \ddots & \vdots \\ \beta_{n1} & \beta_{n2} & \beta_{n3} & \dots & 0 \end{bmatrix}_{t=2} \dots \begin{bmatrix} 0 & \beta_{12} & \beta_{13} & \dots & \beta_{1n} \\ \beta_{21} & 0 & \beta_{23} & \dots & \beta_{2n} \\ \vdots & \vdots & \vdots & \ddots & \vdots \\ \beta_{n1} & \beta_{n2} & \beta_{n3} & \dots & 0 \end{bmatrix}_{t=n_t}$$

108 which represents the gross area changing from one land use to another that year. For example,
 109 β_{23} is the area changing from land-use type 2 to land-use type 3 in km^2 . The transition
 110 matrix at time t can be derived from \mathbf{U}_t by comparison with the previous layer \mathbf{U}_{t-1} . Each
 111 element is given by

$$\beta_{ijt} = \sum_{x=1}^{n_x} \sum_{y=1}^{n_y} [U_{xyt-1} = i \wedge U_{xyt} = j] A_{\text{gridcell}} \quad (3)$$

112 .

113 At each time step, the net change in the area occupied by each land use is given by the gross
 114 gains (the vector of column sums, \mathbf{G}) minus the gross losses (the vector of row sums, \mathbf{L}):

$$\Delta A_{ut} = G_{ut} - L_{ut} \quad (4)$$



115 where

$$G_{ut} = \sum_{i=1}^{n_u} \beta_{iut}$$

116

$$L_{ut} = \sum_{j=1}^{n_u} \beta_{ujt}$$

117 and i and j are the row and column indices.

118 We thus have three data structures, \mathbf{U} , \mathbf{B} , and \mathbf{A} , which are inter-related by equations 1 - 4.

119 \mathbf{U} contains complete information about the system, which can be summarised in the form of

120 \mathbf{A} and \mathbf{B} . \mathbf{B} contains partial information about the system, which can be summarised in the

121 form of \mathbf{A} , but does not directly specify \mathbf{U} . In itself, \mathbf{A} does not directly specify either \mathbf{U} or

122 \mathbf{B} , but can be used as a constraint in their estimation.

123 Multiple data sources are available which provide information in the form of these different

124 data structures. Our approach here is to use equations 1 - 4 as a simple model to relate the

125 different observational data via Bayesian data assimilation in a two-stage process. Firstly, we

126 use a Bayesian approach to estimate the parameters in \mathbf{B} , given prior information and partial

127 observations of \mathbf{U} and \mathbf{A} . Secondly, we use the posterior distribution of \mathbf{B} and spatial and

128 probabilistic information on the location of land-use change to simulate posterior realisations

129 of \mathbf{U} . The maximum *a posteriori* probability (MAP, the mode of the posterior distribution)

130 realisations represent our best estimate of land use and land-use change, given the available

131 data.

132 Data sources

133 We combined a number of data sources (Table 1) to describe the spatial and temporal

134 change in land use in Scotland in the approach outlined above. A classification scheme was

135 produced for each of these to aggregate the data into the broad classes used by Bradley *et al.*

136 (2005 - forest, crop, grassland, rough grazing, urban, and other), close to the IPCC land-use



137 classes (Penman *et al.*, 2003). This was considered coarse enough that differences between
 138 classifications could be aggregated into these six common classes, so that translation between
 139 classifications did not cause major problems. In this classification, “grassland” comprises
 140 all improved and actively managed agricultural grassland. “Rough grazing” comprises all
 141 unmanaged grassland and semi-natural land. All spatial data were rasterised on a common
 142 100-m resolution grid, defined in the GB Ordnance Survey transverse Mercator projection.
 143 The time domain considered was 1969 to 2015.

Abbreviation	Data source	Data structures	Temporal coverage
CS	Countryside Survey	B	1978, 1984, 1990, 2000, 2007
AC	Agricultural Census	A	1969-2016
EAC	EDINA Agricultural Census	G, L, w	1969-2016
Corine	Corine	U, B, w	1990, 2000, 2006, 2012
IACS	Integrated Administration and Control System	U, B, w	2004-2015
NFEW	FC National Forest Estate and Woodlands	U, B, w	1969-2014
FC	FC new planting	G_{forest}	1969-2016
LCM	CEH Land Cover Map	A_{urban}, U, w	1990, 2000, 2007, 2015
ALCM	Agricultural Land Capabil- ity Map	w	NA

Table 1: Data sources assimilated in the estimation of land-use change in Scotland.

144 Data assimilation

145 Our data assimilation method proceeded as follows.

- 146 • From repeat ground-based surveys, the CEH Countryside Survey (CS, Norton *et al.*,
 147 2012; Wood *et al.*, 2017) provides direct observations of **B** for approximately 150 1-km²
 148 survey squares in Scotland. Whilst the coverage is not large compared to the total area
 149 of Scotland, the sample squares were chosen on a stratified design, and the observations
 150 are valuable in having consistent recording methods over a long time period. The
 151 method for scaling these survey squares to national scale is described in (Milne &



152 Brown, 1997). Surveys were carried out in 1978, 1984, 1990, 2000, and 2007, and we
 153 interpolated linearly between survey years to produce an annual time series. We used
 154 the estimates derived in this way as our prior distribution of \mathbf{B} . Each year, the mean of
 155 the prior distribution was taken to be the value of \mathbf{B} from CS. The standard deviation
 156 σ of the prior distribution was estimated by applying a bootstrapping approach to the
 157 CS data (Scott, 2008).

158 • National Agricultural Census (AC) data provide annual records of the total area in
 159 the main agricultural land uses (Scottish Government, 2017). The Agricultural Census
 160 is conducted in June each year by the government agriculture department. Farmers
 161 declare the agricultural activity on their land in the form of ca. 150 items of data via a
 162 postal questionnaire. The results are collated at national scale. These are a long-running
 163 data set with near-complete coverage of agricultural land, relatively consistent over
 164 time, and are reported as national statistics and to the FAO. Hence it is desirable for
 165 our estimates of land-use change to be consistent with these data as far as possible. We
 166 therefore use these data as observations of A_{ut} in the Bayesian framework, and predict
 167 ΔA_{ut} from \mathbf{B}_t according to equation 4. The likelihood of the net change observed by
 168 Agricultural Census ($\Delta A_{ut}^{\text{obs}}$) arising from normal distributions with means determined
 169 by equation 4 and the parameter matrix \mathbf{B} is

$$\mathcal{L}_{\text{net}} = \prod_{t=1}^{n_t} \prod_{u=1}^{n_u} \frac{1}{\sigma_{ut}^{\text{obs}} \sqrt{2\pi}} \exp(-(\Delta A_{ut}^{\text{obs}} - \Delta A_{ut}^{\text{pred}})^2 / 2\sigma_{ut}^{\text{obs}2}) \quad (5)$$

170 where $\Delta A_{ut}^{\text{pred}}$ is the prediction from equation 4 for the change in land use u at time t , and
 171 σ_{ut}^{obs} is the observational error in the Agricultural Census. So, we now have (i) a simple model
 172 which predicts net land-use change in terms of a parameter matrix; (ii) prior estimates of
 173 these parameters for each year from the Countryside Survey; and (iii) a function (equation 5)
 174 for the likelihood of the observations of net change given the model parameters. Combining



175 these in Bayes Theorem, we can estimate the posterior distribution of the parameters, the
176 transition matrix \mathbf{B} . However before describing this, we can extend this simplest likelihood
177 function by adding further sources of observational data.

178 • The EDINA Agricultural Census (EAC) data (<http://agcensus.edina.ac.uk/>) provide
179 additional information on land-use change, as they attempt to produce a spatially explicit
180 version of the national-scale Agricultural Census data. Farm-level data is aggregated
181 to 2-km grid cells, and data are available (or can be inferred) annually. While not
182 containing explicit information on the actual land-use transitions, the resolution of the
183 data is high enough that the net changes recorded each year in each 2-km cell may
184 approximate the gross changes. In other words, because the data records the annual
185 increases and decreases in land use across the grid of 2-km cells, the national totals of
186 these increases and decreases gives an estimate of the gross change, the row and column
187 sums of the transition matrix \mathbf{B} , as well as the net change. When calculating the
188 likelihood in our Bayesian framework, we can thus use the more informative observations
189 of gross gains and losses (\mathbf{G} and \mathbf{L}) rather than just the observations of net change
190 ($\Delta\mathbf{A}$) from the national Agricultural Census. However, we know that the observations
191 will tend to underestimate the gross change, because of the nature of the data reporting
192 process: any counter-balancing gross change within the 2-km square is not included. To
193 account for this, we can use a skewed normal distribution to represent this, such that
194 predictions which overestimate the observations are more likely than underestimates.
195 A skewed normal distribution of this form (Azzalini, 2017) gives the likelihood of the
196 gross changes observed as:



$$\mathcal{L}_{\text{gross}} = \prod_{u=1}^{n_u} \frac{2}{\sigma_{L_{ut}^{\text{obs}}}} \phi \left(\frac{L_{ut}^{\text{obs}} - L_{ut}^{\text{pred}}}{\sigma_{L_{ut}^{\text{obs}}}} \right) \Phi \left(\alpha \left(\frac{L_{ut}^{\text{obs}} - L_{ut}^{\text{pred}}}{\sigma_{L_{ut}^{\text{obs}}}} \right) \right) \times \frac{2}{\sigma_{G_{ut}^{\text{obs}}}} \phi \left(\frac{G_{ut}^{\text{obs}} - G_{ut}^{\text{pred}}}{\sigma_{G_{ut}^{\text{obs}}}} \right) \Phi \left(\alpha \left(\frac{G_{ut}^{\text{obs}} - G_{ut}^{\text{pred}}}{\sigma_{G_{ut}^{\text{obs}}}} \right) \right) \quad (6)$$

197 where ϕ is the standard normal probability density function, Φ is the corresponding cumulative
 198 density function, and α is the skew parameter. Positive α produces a positive skew (when
 199 $\alpha = 0$ we have the standard normal distribution). The parameter α can itself be estimated
 200 as part of the data assimilation procedure.

- 201 • Several data sources provide observations of \mathbf{U} for one or more land uses at a restricted
 202 set of time points. We combine these into a single array \mathbf{U}^{obs} as follows.
 - 203 – For an initial estimate of \mathbf{U} , we use the Corine data sets for 1990, 2000, 2007, and
 204 2012 (European Environment Agency, 2016). For each grid cell, change between
 205 these years was assumed to occur at a random time within the interval, so that at
 206 national scale we effectively interpolate linearly. This produces \mathbf{U} with complete
 207 UK coverage at annual resolution over the period 1990 to 2012.
 - 208 – We overlay this with IACS data over the period 2004 to 2015 (Tomlinson *et al.*,
 209 2017). The Integrated Administration and Control System (IACS) is a European-
 210 wide spatially explicit dataset at the field level that serves as a register of agricul-
 211 tural subsidy claims under the EU Common Agricultural Policy. IACS records
 212 field-level land use (crop type, grassland age, forest coverage), field geometry and
 213 its association to a farm holding. This has large, but not complete spatial coverage
 214 (65 % of the Scottish land area), and the Corine data are retained where IACS
 215 data are missing. Where there are conflicts with Corine, IACS data are given
 216 precedence because they are direct ground-based records.
 - 217 – We then add forestry data from the GB Forestry Commission (FC) National



218 Forest Estate and Woodlands (<https://www.forestry.gov.uk/datadownload>), which
 219 records the location and planting date of forestry. Again, this only has limited
 220 coverage, as it only covers forest land, but is given precedence in the case of conflict
 221 with the Corine/IACS data. We iterate over each time step to calculate $\mathbf{B}_t^{\text{obs}}$ with
 222 equation 3. $\mathbf{B}_t^{\text{obs}}$ thus contains an observed estimate of the transition matrix for
 223 each year, from the combination of Corine, IACS and FC data.

224 We can therefore add an additional term to the likelihood function which incorporates the
 225 comparison of the observations \mathbf{B}^{obs} with the values in the current parameter set \mathbf{B}^{pred} .

226

$$\mathcal{L}_{\mathbf{B}} = \prod_{\substack{i=1 \\ j=1 \\ t=1}}^{\substack{n_u \\ n_t}} \frac{1}{\sigma_{\beta_{ijt}^{\text{obs}}} \sqrt{2\pi}} \exp\left(-(\beta_{ijt}^{\text{obs}} - \beta_{ijt}^{\text{pred}})^2 / 2\sigma_{\beta_{ijt}^{\text{obs}}}^2\right) \quad (7)$$

- 227 • To establish the posterior distribution, we use the Markov Chain Monte Carlo (MCMC)
 228 approach with the “DEz” algorithm implemented in the R package `BayesianTools`
 229 (Hartig *et al.*, 2017). For each interval in the 46 year time series, an MCMC simulation
 230 was run, using the prior \mathbf{B}_t matrix from Countryside Survey, the observations of $\Delta\mathbf{A}_t$,
 231 \mathbf{L}_t , \mathbf{G}_t for that year, and the observed \mathbf{B}_t matrix from Corine-IACS_NFEW. In practice,
 232 it is more convenient to use log-likelihoods, and our overall likelihood was the summation
 233 of $\log(\mathcal{L}_{\text{net}})$, $\log(\mathcal{L}_{\text{gross}})$ and $\log(\mathcal{L}_{\mathbf{B}})$. Nine chains were used, with 100,000 iterations in
 234 each. To establish the initial \mathbf{B} parameter values for one of the chains, a least-squares fit
 235 with the $\Delta\mathbf{A}$ was used. Other chains were over-dispersed by adding random variation
 236 to this best-fit parameter set.
- 237 • Having established the posterior distribution of \mathbf{B} , we use spatial and probabilistic
 238 information on the location of land-use change to simulate posterior realisations of
 239 \mathbf{U}^{post} . Starting with our best estimate of the near-present state of land use, $\mathbf{U}_{t=2015}^{\text{obs}}$,
 240 we work backwards in time. At each time step, we know the number of grid cells which



241 need to change from land use i to land use j from the posterior matrix \mathbf{B}_t . For each i
 242 to j transition, we perform a weighted sampling operation to select this number of cells
 243 from those where $U_{xyt} = i$. In choosing which cells to assign to j , we use the available
 244 data to calculate the probabilities which weight the sampling. Recall that \mathbf{U}^{obs} is given
 245 by the amalgamation of Corine, IACS and NFEW data. In the simplest case, the
 246 probabilities are determined only by this: all cells where $U_{xyt}^{\text{obs}} = i$ and $U_{xy,t-1}^{\text{obs}} = j$ have
 247 equally high probability of being selected in the sample, and all cells where $U_{xyt}^{\text{obs}} = i$
 248 and $U_{xy,t-1}^{\text{obs}} \neq j$ have equally low (but non-zero) probability of being selected in the
 249 sample. This requires only a few simple rules to construct the probability weightings,
 250 w , for sampling cells for conversion from i to j :

$$\begin{aligned} & \text{if } U_{xy,t}^{\text{obs}} \neq i \text{ then } w_{xy} \leftarrow 0 \text{ else } w_{xy} \leftarrow 1 \\ \wedge & \text{ if } U_{xy,t-1}^{\text{obs}} = j \text{ then } w_{xy} \leftarrow 1 \text{ else } w_{xy} \leftarrow p_m \end{aligned}$$

251 where p_m is the probability of cells being misclassified in \mathbf{U}^{obs} , which we estimate to be
 252 0.05. Sampling is done without replacement, so that a grid cell can only be selected
 253 once per year. To illustrate with an example, we start with our current map of land
 254 use, $\mathbf{U}_{t=2015}^{\text{obs}}$. Suppose our posterior estimate of \mathbf{B}_t determines that seven grid cells
 255 change from crop to grass, as we go back to 2014. Only cells which are crop in 2015 are
 256 valid candidates. Of these, those which were grass in 2014 (according to \mathbf{U}^{obs}) will have
 257 high probability of being selected; others will have a low probability. If the posterior
 258 $\beta_{ijt}^{\text{post}}$ area is lower than β_{ijt}^{obs} , not all the cells with high weightings from the above rules
 259 will be selected in the sample. If the posterior $\beta_{ijt}^{\text{post}}$ area is higher than β_{ijt}^{obs} , additional
 260 cells, with low weightings from the above rules, will be selected in the sample. Thus,
 261 the cells which we are likely to change are those which are designated by \mathbf{U}^{obs} as crop
 262 in 2015 and grass in 2014. The effect of this is to generally recreate the spatial and



263 temporal pattern seen in \mathbf{U}^{obs} (data from Corine, IACS and NFEW), but modified
264 according to the extent of change estimated in the posterior \mathbf{B}^{post} .

265 • As well as using the data from Corine, IACS and NFEW, we can also use other spatial
266 data sets to inform the location of land-use change in our simulations of the posterior
267 U_{xyt} . Any spatial data set which gives information on where and when a land use or
268 land-use change occurs can be incorporated into the weighting used for sampling. Here,
269 we used three additional data sets.

270 – EDINA Agricultural Census gives an estimate of $\Delta\mathbf{A}$ at 2-km resolution. For each
271 land use, an observed increase in area indicates the likely location of predicted
272 gains. We therefore add a term to w which is proportional to $\Delta\mathbf{A}$.

273 – The CEH Land Cover Map (Rowland *et al.*, 2017) gives an estimate of \mathbf{U}_t in 1990,
274 2000, 2007, and 2015 at high spatial resolution. Occurrence of a land use in the
275 LCM suggests an area where gains would be more likely to occur. We add a term
276 to w , based on occurrence of that land use in the LCM.

277 – Agricultural Land Capability Maps gives an estimate of how suitable land is for
278 intensive agriculture, with a scale which ranges from good arable land, through
279 intensive grassland and extensive grassland, to rough grazing. This scale can be
280 translated into a probability of occurrence for the land uses considered here, and
281 added into the weighting of the sampling again. We use all the above information
282 to produce many posterior realisations of \mathbf{U}^{post} , using the posterior B matrix and
283 the sampling process described earlier.

284 Because the \mathbf{U} data structure is large, we are limited in simulating many samples. It is
285 therefore useful to summarise as the much smaller set of unique vectors and their corresponding
286 areas. Our approach is to simulate 1000 samples, to calculate the unique vectors and their
287 areas, and not to retain the larger data structure to reduce storage requirements. Another
288 possible approach would be to simulate using only the MAP B matrix, and thereby generate
289 the most likely realisations of U_{xyt} , rather than the whole posterior distribution.



290 Carbon dynamics following land use change

291 We applied a simple empirical model of carbon fluxes following land use change, based on the
292 UK LULUCF GHG inventory (Griffin *et al.*, 2014). The soil component is based on the work
293 of Bradley *et al.* (2005), and uses an analysis of the total soil carbon stock in a large number
294 of soil cores, classified by land use and soil series. A linear mixed-effects model was applied
295 to these data, to quantify the average effect of land use on soil carbon stock, treating soil
296 series as a random effect. The model uses these mean values to represent the equilibrium soil
297 carbon stock for each land-use class. When land use changes, the soil carbon stock moves
298 towards the equilibrium soil carbon stock for the new land use. The soil carbon stock at
299 location (x,y) and time t is given by:

$$C_{xyt} = C_u^{\text{eq}} - (C_u^{\text{eq}} - C_{xy,t-1}) \exp(-k\Delta t) \quad (8)$$

300 where C_u^{eq} is the equilibrium soil carbon stock for the current land use u , $C_{xy,t-1}$ is the soil
301 carbon stock at the previous time step, and k is a rate constant. The flux of carbon over the
302 time step, Δt , is given simply by difference:

$$F_C = C_{xyt} - C_{xy,t-1} \quad (9)$$

303 The above-ground component applies to the growth of biomass following afforestation, and uses
304 the yield tables for British forestry produced by Edwards & Christie (1981), as interpolated
305 and expanded to include non-merchantable timber biomass and wood products by Dewar &
306 Cannell (1992). The mean change in above-ground biomass was assumed to be negligible in
307 other land-use transitions in this simple model.



308 Results

309 Because of the availability of remotely-sensed data products, we are relatively confident in
310 the present-day distribution of land use (Figure 2). This shows the concentration of urban
311 areas in Scotland in the central belt, the restriction of cropland to the drier, flatter east coast,
312 improved grassland mainly in the lowlands in the wetter south and west, and rough grazing
313 and forestry sharing the Southern Uplands and Highlands in the north and west.

314 As an initial step in the data assimilation process, a close least-squares fit to $\Delta\mathbf{A}$ was
315 achieved within a few tens of iterations, indicating that there were no particular numerical
316 difficulties in estimating the \mathbf{B} parameters. Standard measures were applied to assess whether
317 the posterior distribution of \mathbf{B} was suitably characterised by the output of the MCMC
318 sampling. As well as inspection of the trace plots and the form of the distribution of the \mathbf{B}
319 parameters, we calculated the effective sample size, the acceptance rate, and various
320 standard convergence diagnostics (Gelman & Rubin, 1992; Geweke, 1992; Raftery & Lewis,
321 1992). All of these showed satisfactory performance, that the MCMC chains converged,
322 and that nine chains with 100,000 samples provides a reasonable estimate of the posterior
323 distribution of \mathbf{B} .

324 Figure 3 shows the Agricultural Census observations, and posterior predictions of the net
325 change in area of each land-use class. The net change implied by the prior CS and IACS
326 observations of \mathbf{B} are also shown. The broad trends are: (i) an increase in forest cover due
327 to sustained commercial forest planting; (ii) a corresponding decrease in rough grazing and
328 semi-natural land due to expansion of forestry and improved grassland; (iii) an increase in
329 cropland area between 1970 and 1990, with subsequent decline to the present day, due to
330 changes in economic forces and subsidy incentives; (iv) an increase in grassland area since
331 around 1990, partly corresponding to the reduction in crop area, and partly due to a general
332 expansion on to rough grazing areas; and (v) a slow but consistent expansion of the urban
333 area. These trends are picked up by the different sources of observations to some extent. The

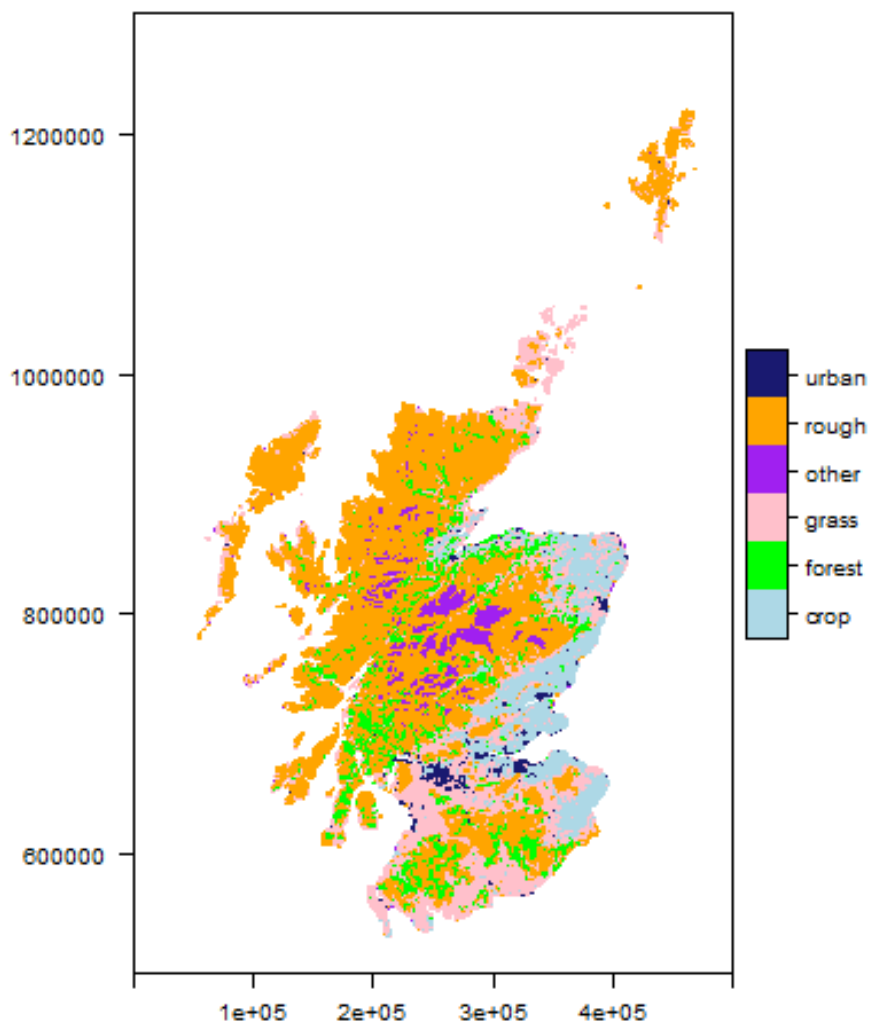


Figure 2: Land use in Scotland in 2015 as estimated by the CEH Land Cover Map. “Grass” comprises all improved and actively managed agricultural grassland. “Rough” includes all rough grazing, unmanaged grassland and semi-natural land. “Other” comprises barren areas such as montane and coastal areas. For legibility, we show this aggregated to 2-km squares, though the data are available at 250-m resolution

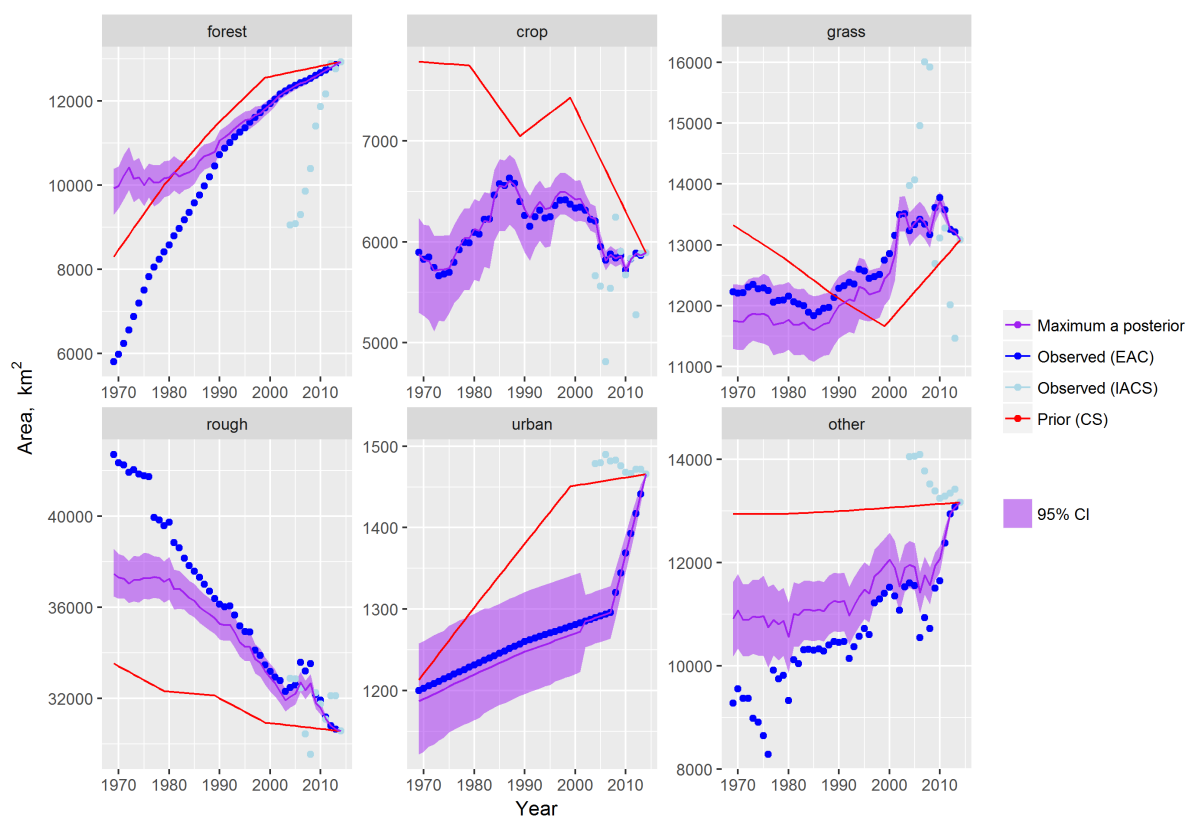


Figure 3: Time series of the area occupied by each land use (A_{ut}) from 1969 to 2015, showing the observations, prior and posterior estimates. The shaded band shows the 2.5 and 97.5 % percentiles of the posterior distribution of the net change in area.



334 Agricultural Census has near-complete coverage, and annual resolution, so shows a detailed
 335 pattern, to which we give most credence. The CS data, used as the prior, have only decadal
 336 time resolution, but pick up these general trends, and approximate the same pattern as seen
 337 in the Agricultural Census data. The IACS data show considerable year-to-year variability,
 338 and tend to show exaggerated net changes compared to AC. The posterior prediction generally
 339 falls in between the AC observations and the CS prior, but tracks closer to the AC.

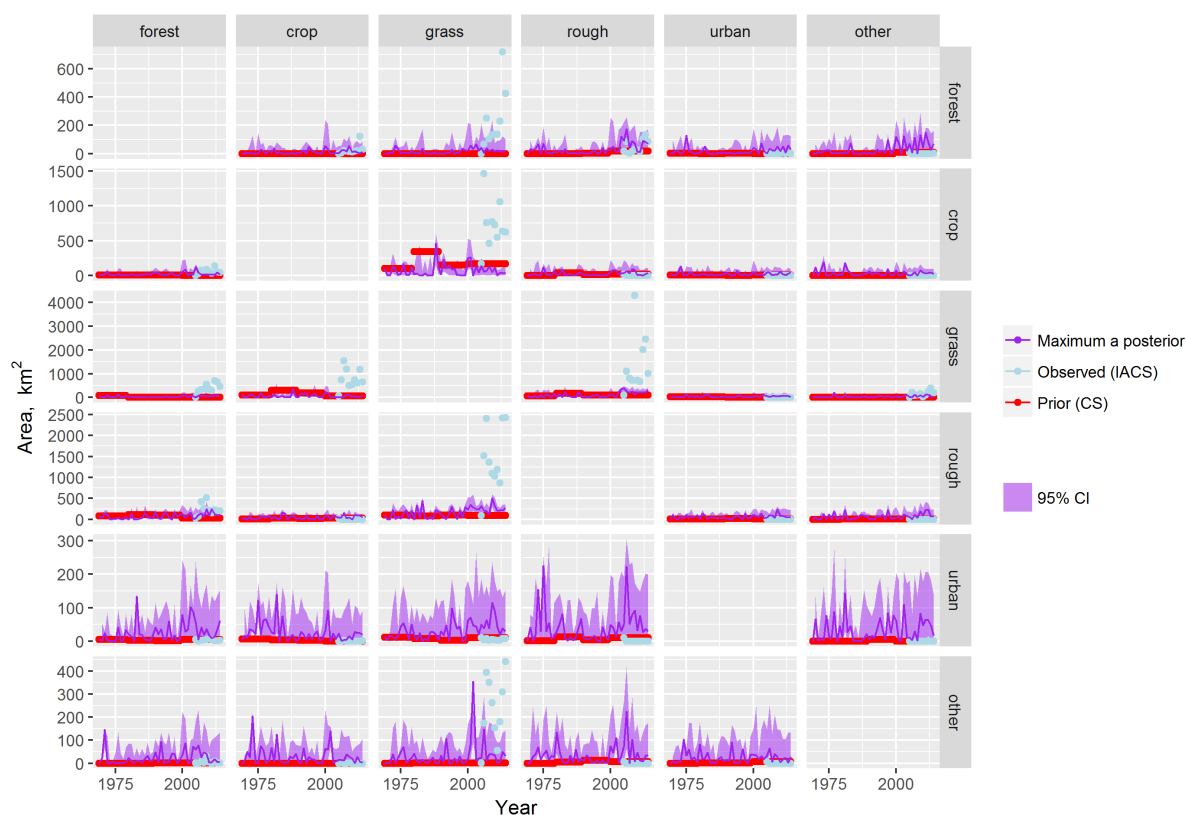


Figure 4: Prior and posterior distributions of the transition matrix \mathbf{B} , representing the gross area changing from the land use in each row i to the land use in each column j each year from 1969 to 2015. Red lines show the prior estimate from the Countryside Surveys. Pale blue points show estimates from IACS plus Corine and NFEW. The maximum *a posteriori* estimates after assimilating all data sources are shown in purple. The shaded band shows the 2.5 and 97.5 % quantiles of the posterior distribution. Note the y scale is different for each row.

340 CS provided our prior estimate of \mathbf{B} . Given the relatively small spatial coverage of CS,



341 uncertainty (σ) in the prior \mathbf{B} is rather high. This would be expected to effectively limit the
342 influence of the prior on the posterior \mathbf{B} , compared to the observations from IACS, which
343 have national coverage. Figure 4 shows that estimates of \mathbf{B} from these two data sources are
344 quite different. Particularly in the transitions to and from grassland, values of \mathbf{B} from IACS
345 tend to be an order of magnitude larger than values from CS, and more variable. However,
346 the posterior \mathbf{B} remains closer to the prior than might be expected. This is because values of
347 \mathbf{B} close to the IACS observations are deemed unlikely with respect to the other terms in the
348 likelihood function. That is, the gross and net changes in area implied by the IACS data are
349 inconsistent with the other observations of \mathbf{G} , \mathbf{L} and $\Delta\mathbf{A}$ from AC (Figures 3 - 6).

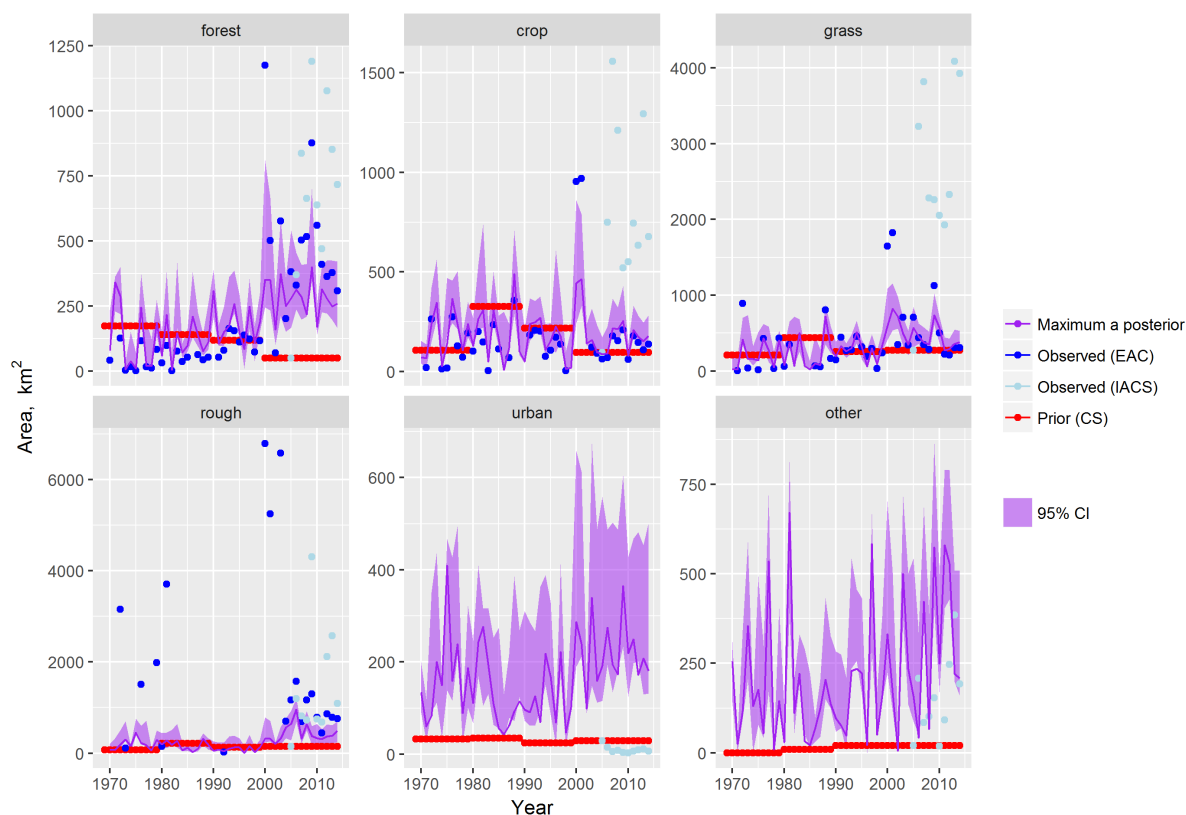


Figure 5: Time series of the gross gain in area of each land use (A_{ut}) from 1969 to 2015, showing the observations, prior and posterior estimates. The shaded band shows the 2.5 and 97.5 % percentiles of the posterior distribution.

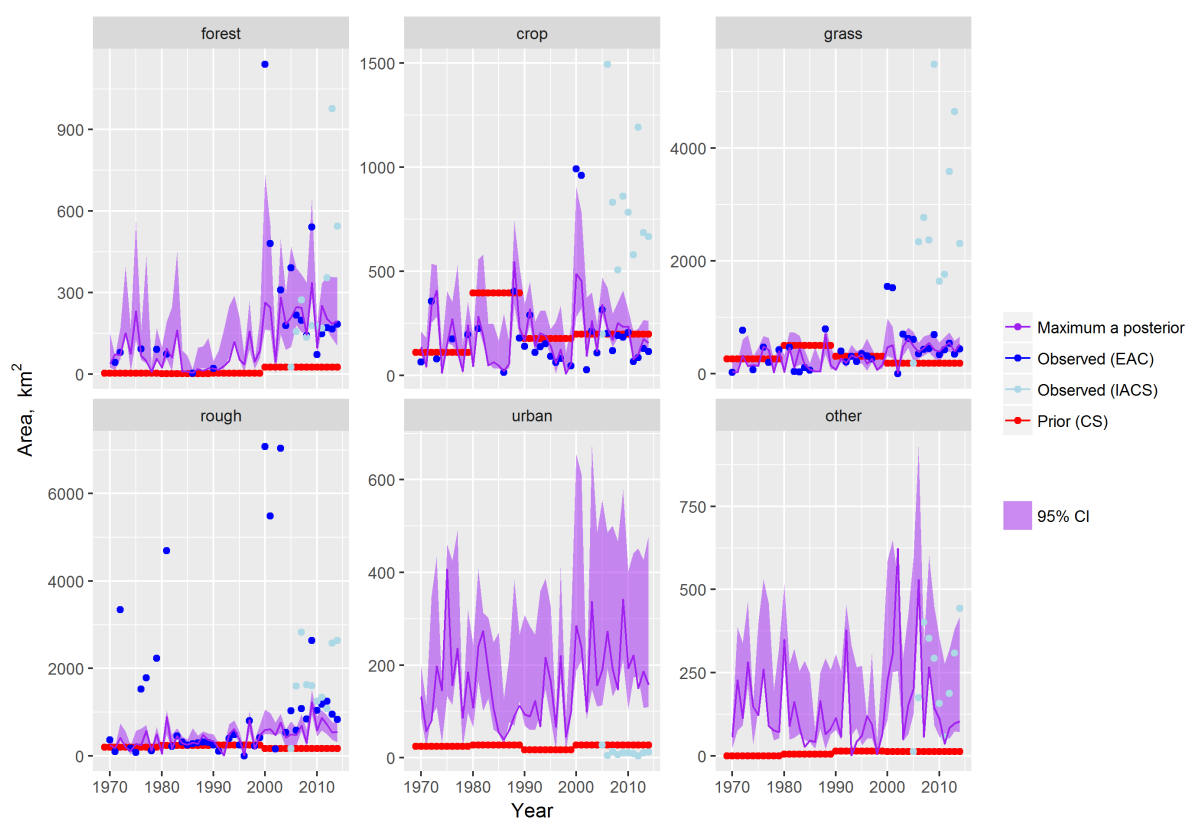


Figure 6: Time series of the gross loss in area from each land use (A_{ut}) from 1969 to 2015, showing the observations, prior and posterior estimates. The shaded band shows the 2.5 and 97.5 % percentiles of the posterior distribution.



350 For cropland and improved grassland, CS and EAC show general agreement on the magnitude
351 and pattern in area gained and lost to each land use (Figure 5 and Figure 6). An exception
352 is an apparent anomaly in the early 2000s, when EAC gains and losses are both around 1000
353 km² higher than average for two years. This is not reflected in the net changes reported in
354 the AC, so has to be treated with some caution. Reported gains and losses of rough grazing
355 are much higher and very variable in EAC. This variability does not seem closely linked to
356 the net change reported at national scale, so again, we treat this with some scepticism. There
357 are no data on the gross gains and losses of urban and other land-use areas, as they are not
358 covered by the AC or CS, and these terms are less well constrained.

359 Figures 3 - 6 show that there is considerable spread in the posterior distribution of **B** and
360 predictions of $\Delta\mathbf{A}$. The 95 % credibility interval is typically of the order of 100 km² for the
361 individual **B** parameters, and several hundred km² for the predictions of $\Delta\mathbf{A}$. The credibility
362 intervals are smallest where multiple data sources agree on the nature of land-use change,
363 and where the change is coherent across land uses. That is, an increase in one land use
364 has to be balanced by a decrease in one or more other land uses. We have less confidence
365 in predictions where the observed change in one land use is not compensated for by other
366 land use changes. Credibility intervals in $\Delta\mathbf{A}$ increase as we go back in time, because the
367 uncertainty accumulates from year to year, although the increase has square root form rather
368 than linear,

369 Figure 7 and Figure 8 attempt to convey the detailed structure of the posterior **U** in a simple
370 graphical summary. Figure 7 shows the 100 most frequent vectors of land-use change. Line
371 thickness and opacity are proportional to the frequency (= area) of each vector, so that
372 the dominant vectors are the most visually obvious. The plot shows that a wide range of
373 land-use transitions occurs over the time period considered. Transitions from rough grazing
374 to forest and to improved grassland are dominant. Bi-directional transitions between crop
375 and improved grassland are particularly common in the 1980s. This comes from information

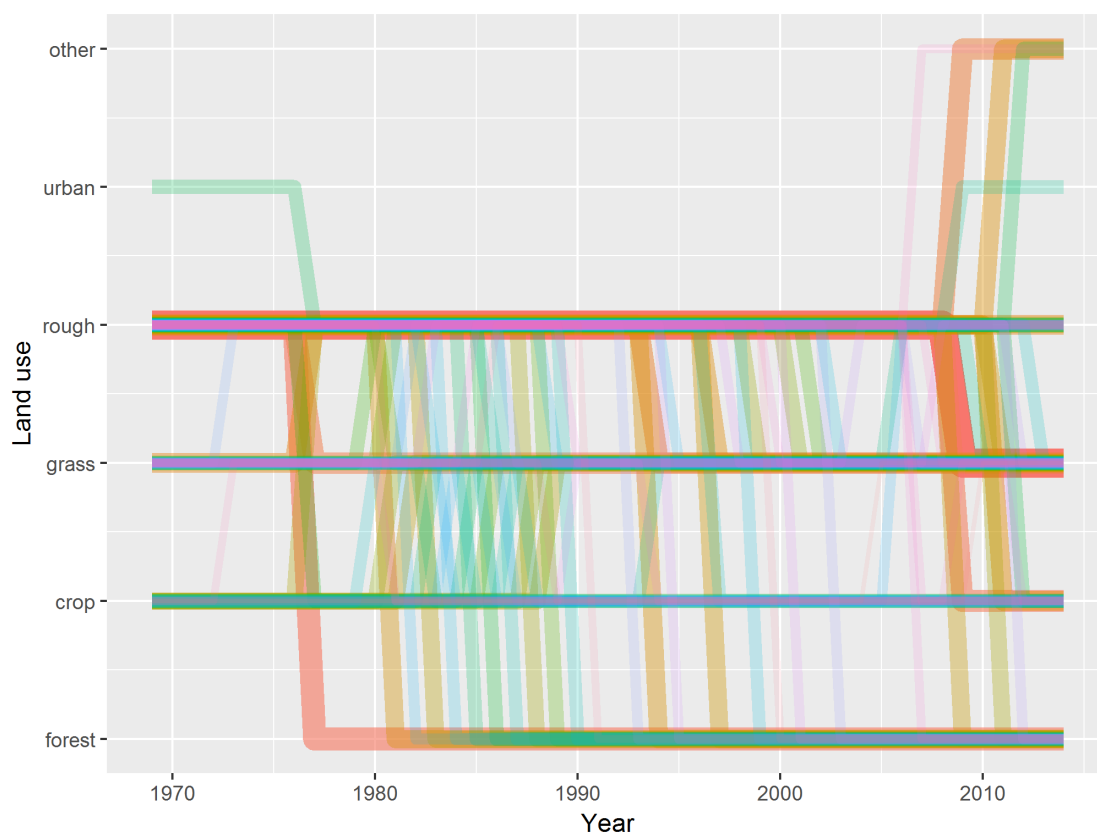


Figure 7: Trajectories of the 100 land-use vectors in the posterior U with the largest areas (excluding the six vectors which show no change). Each vector of land use is shown in a different colour, varied arbitrarily to differentiate different vectors. Line thickness and opacity are proportional to the frequency of (or total area occupied by) each vector, so that the dominant vectors are the most visually obvious.

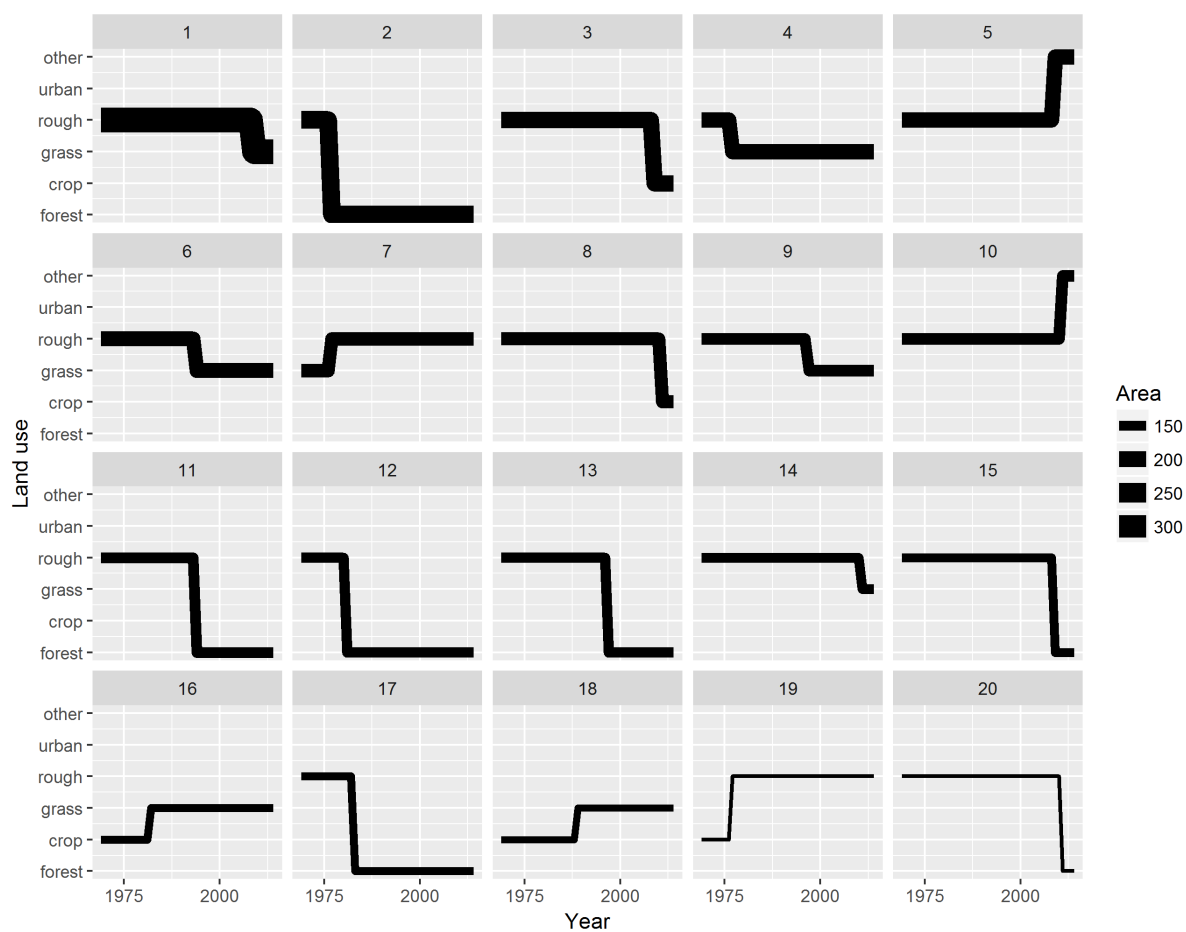


Figure 8: Trajectories of the 20 land-use vectors in the posterior U with the largest areas (excluding the six vectors which show no change). Line thickness is proportional to the frequency of (or total area occupied by) the vector



376 in the prior, the **B** matrices from CS which shows markedly higher crop to grass and grass to
377 crop conversion rates over this time.

378 Figure 8 shows the 20 most frequent vectors more clearly, with each vector on a separate
379 panel. This shows that 17 out of 20 involve transitions to or from rough grazing (which
380 includes all semi-natural) land, which is the largest land use in Scotland by some way (around
381 half the total area). Seven of these represent afforestation, which has mainly occurred on
382 less productive, upland rough grazing land. Five vectors represent expansion of improved
383 grassland on to rough grazing land. Vectors with two or more changes are less frequent, with
384 none occurring in the top 20, but do represent a significant part of the total area (~8 % of
385 the area undergoing change).

386 Figure 9 shows the CO₂ flux resulting from land-use change over the 46-year period, derived
387 from equations 8 - 9 and the posterior distribution of **U**. The positive fluxes denote a
388 gain to the terrestrial carbon stock, negative fluxes represent a loss to the atmosphere. We
389 only represent land-use change from 1969 onwards here, but the effects on carbon flux are
390 long-lasting. Hence, the carbon flux calculated here is initially small, and increases as the
391 area having undergone land-use change accumulates over time. The accumulation of carbon
392 in forest biomass (and wood products) following afforestation over this period is the largest
393 term in these results. The forest planting rate has decreased markedly since 2005, giving the
394 reduction in carbon sequestration in recent years. In this simple soil model, land uses with
395 higher equilibrium soil carbon than the average will tend to act as carbon sinks; those lower
396 than the average will be sources. Carbon emissions from cropland increase as predominantly
397 grassland is converted to cropland between 1970 and 1990. This then levels off as the cropland
398 area remains stable or declines thereafter. Transitions to forest and rough grazing result in
399 carbon sinks because they both have higher than average equilibrium soil carbon, and both
400 show sizeable gross gains over the period. Rough grazing land also shows substantially larger
401 gross area losses, but the associated carbon fluxes associated with this are attributed mainly

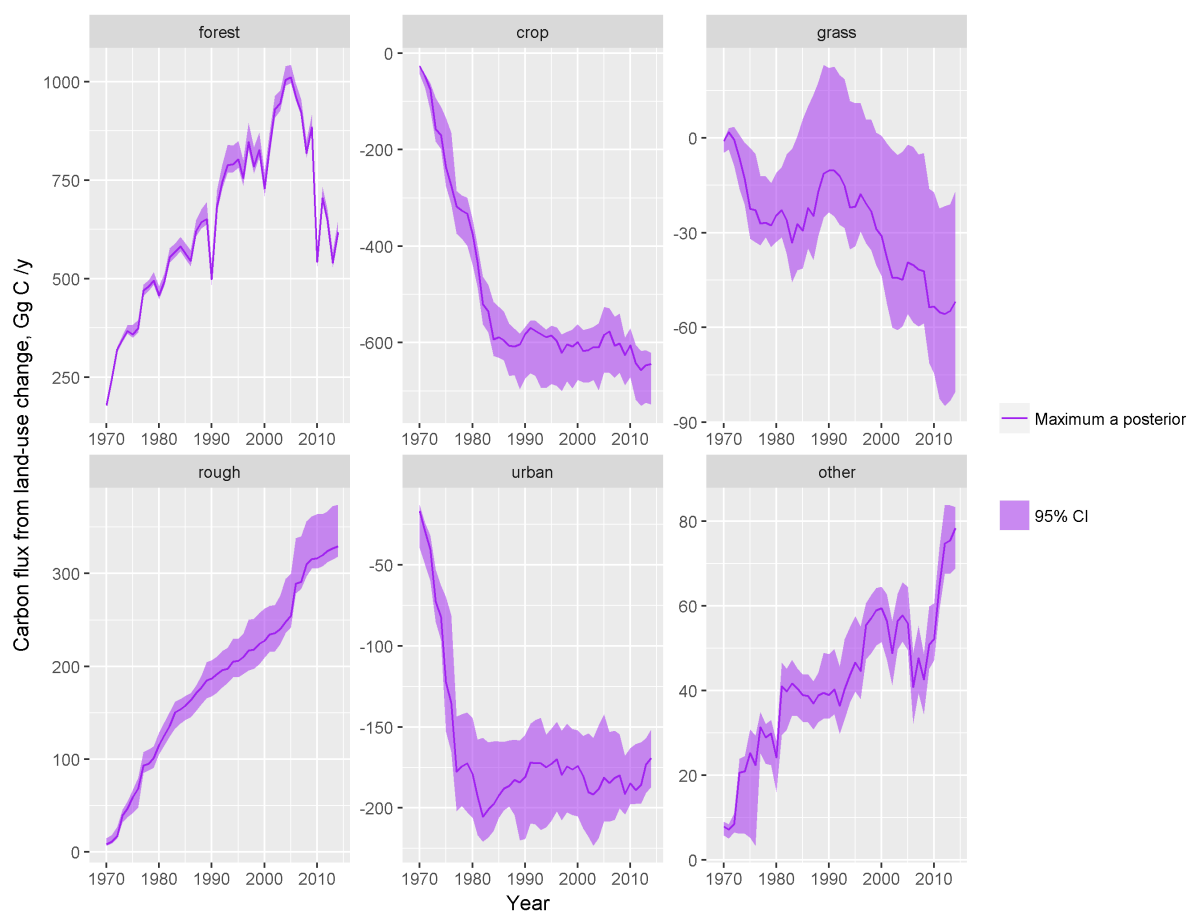


Figure 9: Net carbon flux from land-use change in Scotland over 1969-2015 showing the maximum *a posteriori* estimate and its 95 % credibility interval. The flux is attributed to change to each land-use class *u*. Positive fluxes denote a gain to the terrestrial carbon stock; negative fluxes represent a loss to the atmosphere.



402 to improved grassland, as this is the main land use to which it changes. Improved grassland
403 therefore shows as a small net source of carbon, the result of land use changes from cropland
404 to improved grassland (sink) and rough grazing to improved grassland (source).

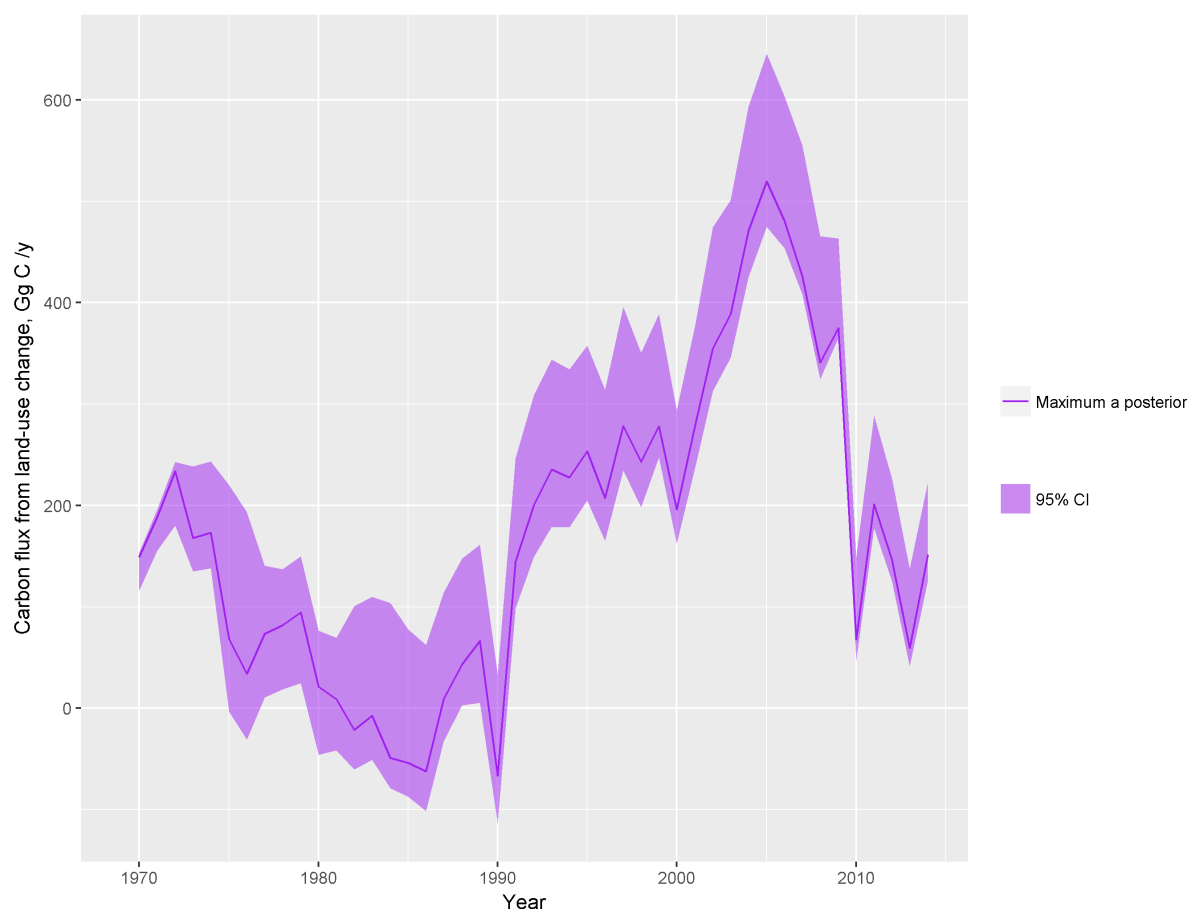


Figure 10: Total net carbon flux from land-use change in Scotland over 1969-2015, showing the maximum *a posteriori* estimate and the 95 % credibility interval. Positive fluxes denote a gain to the terrestrial carbon stock; negative fluxes represent a loss to the atmosphere.

405 The overall effect of these component fluxes is to produce a net sequestration of carbon
406 from land-use change (Figure 10). The 95 % credibility interval in the near-present-day
407 carbon flux is around 100 Gg C y^{-1} , close to 50 % of the best estimate. There is therefore
408 considerable uncertainty in the carbon flux associated with land-use change, because the



409 underlying changes in land use are themselves uncertain. Recognition and propagation of
410 this uncertainty is therefore important.

411 Mapping the carbon fluxes calculated by equations 8 - 9 and the MAP estimate of \mathbf{U} , we
412 can see that the carbon fluxes closely follow the present-day land-use distribution (Figure
413 11). The carbon sinks are associated mainly with new forest areas, and to a lesser extent,
414 wherever improved grassland or cropland has reverted to rough grazing. The carbon sources
415 are associated with wherever cropland or urban areas have expanded.

416 Discussion

417 The results show that we can provide improved estimates of past land-use change using
418 multiple data sources in the Bayesian framework. The computation involved is quite feasible
419 on a modern computer, requiring around three hours to estimate the parameters for a 46-year
420 period. The output of the assimilation procedure provides vectors of land-use change in
421 the form required for dynamic and process-based modelling, which we illustrate with the
422 soil carbon modelling example. The main advantage of the approach is that it provides a
423 coherent, generalised framework for combining multiple disparate sources of data.

424 As far as we are aware, there are no previous applications of formal data assimilation
425 approaches to land-use change. However, some studies have addressed the same problem with
426 related methods. Hurrt et al. (2006, 2011) used estimates of \mathbf{A} together with estimates of
427 wood harvest to predict \mathbf{B} . The study was carried out at global scale at 0.5 degree resolution,
428 and covered both historical and future scenarios for the period 1500-2100. To make the
429 problem tractable, the transition matrix \mathbf{B} was initially specified for only three land uses,
430 so that a unique minimum solution could be found. Additional transitions associated with
431 shifting cultivation and wood harvest were then calculated in a further step. They used a
432 rule-based model which specified assumptions about the residence time of agricultural land,

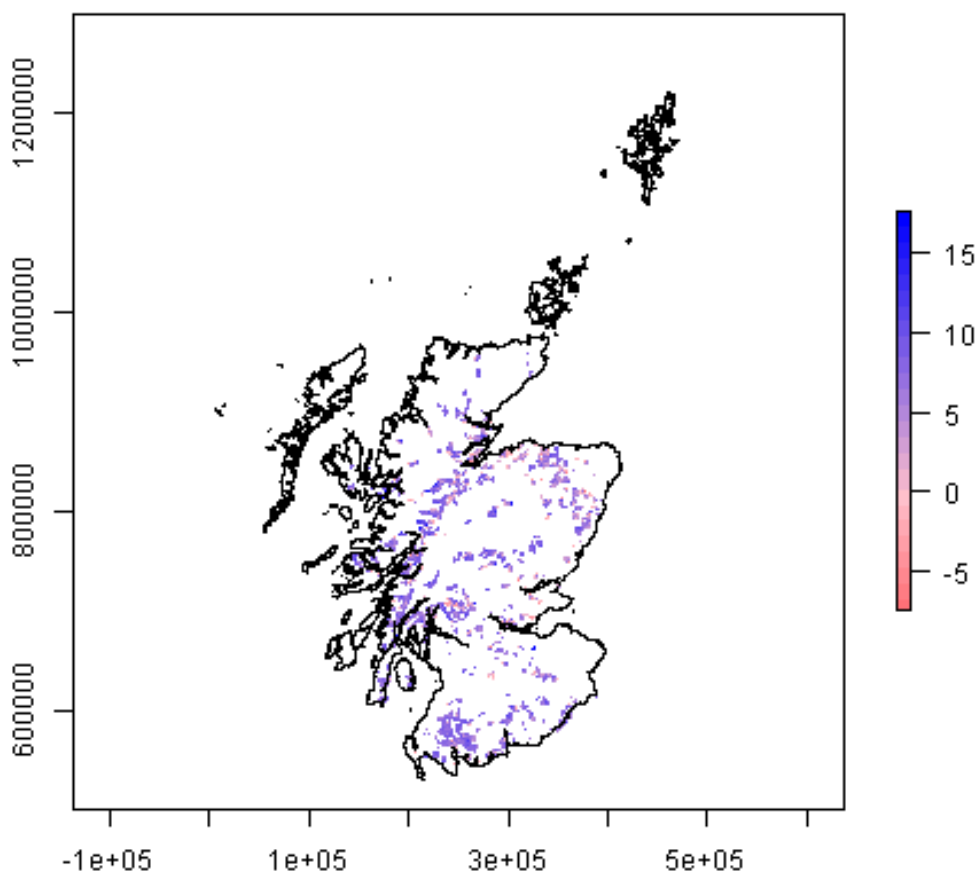


Figure 11: Net carbon flux (in kg C m^{-2}) from land use change in Scotland over 1969-2015 from the maximum *a posteriori* estimate of U . Positive fluxes denote a gain to the terrestrial carbon stock; negative fluxes represent a loss to the atmosphere.



433 the priority of land for conversion to agriculture and for wood harvesting, and the spatial
434 pattern of wood harvesting within a country. The distribution of land use over space and time
435 \mathbf{U} was not explicitly represented; instead, the area and age of “secondary” land in each grid
436 cell was tracked in a book-keeping approach. However, because only a matrix is calculated
437 at each time step, the approach does not produce explicit vectors of land use for dynamic
438 modelling, and such things as rotational land use are not easily represented. Sensitivity to
439 various assumptions was analysed, but the uncertainties associated with the input data and
440 these model assumptions cannot readily be quantified.

441 Fuchs et al. (2013) used a number of data sets, including that of Hurrt et al. (2006), to
442 explicitly estimate the change in land use over space and time \mathbf{U} for the whole of Europe
443 at 1 km² resolution for each decade 1900-2010. Using logistic regression, they calculated
444 “probability maps” for each land cover class, based on biogeophysical and socio-economic
445 properties of each grid cell as explanatory variables for land use in 2000. For each decade
446 and each country within the EU27, the net increase in the area of each land use (positive
447 ΔA_{ut}) was allocated to the grid cells with the highest probability score for that land use.
448 This approach yields essentially the same data structure as our method, and is wider in scope,
449 covering all of Europe.

450 Our method represents an advance on this in several ways. Because the approach of Fuchs
451 et al. (2013) is based on net change in areas at country scale, the extent of the true, gross
452 changes will be under-estimated, possibly by orders of magnitude, and implicitly the \mathbf{B}
453 matrices are minimised. Our approach uses explicit observations of the annual transition
454 matrices \mathbf{B} as far as possible. Rather than regression relationships, our approach uses annual
455 spatially explicit observations of where and when land-use change is likely to have occurred
456 (based on CS, IACS and EAC). We use higher temporal and spatial resolution (annually,
457 at 100 m) because this is possible with the data available in the UK, and with the limited
458 spatial domain we attempt to cover. At continental and global scales, the same quantity and



459 resolution of data is not available, and the computation issues become much larger. Our
460 approach explicitly incorporates and propagates the uncertainty in the posterior distribution
461 of **B** and predictions of **A** and subsequently modelled carbon fluxes. The uncertainty in
462 land-use change is substantial, even in the UK where land management records are good.
463 Our methodology accounts for this uncertainty in a mathematically rigorous way (Van Oijen,
464 2017), and propagates this through to the subsequent modelling of other outputs, such as soil
465 carbon fluxes. On a fundamental level, the Bayesian approach gives the correct theoretical
466 answer to the data assimilation problem: if the observational error and prior are correctly
467 specified and the posterior is adequately characterised by the MCMC sampling, then the
468 posterior correctly represents the actual state of knowledge about the system parameters and
469 predictions (Gelman *et al.*, 2013; Reich, 2015).

470 We thus need to consider how well we can characterise the observational error, and the prior
471 and posterior distributions. Establishing that the posterior distribution has been adequately
472 characterised by the MCMC sampling is relatively straightforward. There are various criteria
473 for assessing this (the effective sample size, and measures of MCMC chain convergence) which
474 the results meet. In this study we chose to use an informative prior based on CS. This follows
475 the way in which the data became available chronologically; these were the only data available
476 with which we could estimate land-use change in the UK when an inventory of carbon
477 emissions was first attempted (Cannell *et al.*, 1999). The uncertainty in the prior distribution
478 of **B** can be relatively well quantified, because considerable effort has gone into quantifying
479 the likely level of error in the national-scale estimates of land use (Scott, 2008; Wood *et*
480 *al.*, 2017). The standard deviation σ of the prior distribution was most easily estimated by
481 applying a bootstrapping approach to the CS data, but more advanced approaches have been
482 investigated (Henry *et al.*, 2015). Alternative options for the prior are possible, and would be
483 worth exploring further to examine sensitivity to the specification of the prior. Where little
484 information is available, an uninformative prior is often used, either uniform, or exponentially
485 declining to capture the parsimony principle that low values of **B** are more likely than high



486 ones, all else being equal. More usefully, because we iterate over all years independently, we
487 could form the prior distribution at time t from the posterior distribution for the previous
488 year. In practice, we iterate backwards in time, so in fact the posterior at time t becomes the
489 prior for time $t - 1$; this is mathematically simple but linguistically confusing. This approach
490 means that information gained in the recent part of the time series is carried over into the
491 earlier part of the time series. Subsequent estimates “borrow strength” from previous ones,
492 in the Bayesian terminology. Currently, we do not use this approach because of the extra
493 computation time this incurs, but methods to speed up this step can be explored.

494 Observational error can be difficult to estimate objectively and accurately, and often the
495 σ terms are poorly known. Even in relative terms, it can be hard to judge the degree of
496 certainty to place in different data sources, where observational error is not readily quantified.
497 In our case, we need to estimate the σ terms in the likelihood function (equations 5 - 7) for
498 the AC, EAC and IACS data. Spatial coverage in the data sets is similarly large so there
499 is no clear *a priori* reason to trust one more than the other. However, there are reasons to
500 prioritise the national-scale trends in AC over those from IACS, and to be cautious of the
501 spatial patterns in EAC. AC is a long-established survey with relatively consistent methods,
502 whereas IACS is a recent introduction, and the recording methodology has not been entirely
503 stable over this period (for example, with changes to how much farm woodland is recorded).
504 It also attempts to collect a much higher level of detail (at the individual field scale), and this
505 brings more potential for misclassification to appear as ostensible land-use change. However,
506 with the limited information available, we cannot rule out that this is the more accurate data
507 set, and that EAC and CS underestimate gross change. The accuracy of spatial information
508 in EAC is limited by the way in which the data are collated, using postcodes of the land
509 owner who completes the census return. Where large estates are owned, the correspondence
510 between the centroid of the postcode district and the actual location of the land may not be
511 very close. We therefore ascribe lowest uncertainty to AC, and higher but equal uncertainty
512 to EAC and IACS data. In our Bayesian data assimilation procedure, IACS-based estimates



513 of **B** are effectively down-weighted when they produce a mismatch with the national-scale
514 AC trends. IACS coverage on forest, urban and other land is not large, and we would not
515 expect accurate detection of changes in these land uses.

516 One of the main problems in land-use studies is that of classification. Depending on definitions
517 used to delimit land-use classes, quite different areas may be calculated for the same nominal
518 classes, and there is a real problem in combining data from different sources in that we
519 may not be comparing like with like. Here, we minimise this problem by using a relatively
520 coarse land-use classification, with only six classes. This would become more problematic if
521 attempting to distinguish more refined classes. The computation time and difficulty increases
522 with the square of the number of land-use classes, so there may be practical limits to the
523 level of detail in the classification used, especially if applying on larger spatial domains.

524 An attractive feature of the Bayesian data assimilation approach is that additional data
525 sources can be added to the process as they become available, without any major changes to
526 software or step-changes in results. Several other data sources exist in the UK which could be
527 incorporated. These include spatial data on the granting of woodland felling licenses, which
528 would further constrain the likely location of deforestation, and national mapping agency
529 data on urban expansion. As new satellite instruments come on-stream (e.g. from Sentinel
530 and synthetic aperture radar), further remotely-sensed data products will become available
531 which could be added into the estimation of **A**, **B** and **U**. In this study, we do not attempt
532 to forecast future land-use change, but in principle this is simple with this methodology. If no
533 new data are available, the posterior distribution will widen as future years are iterated over.
534 If scenario data were supplied, such as projected forest planting rates (G) or cropland areas
535 required for food security (A), these could be used in the estimation of **A**, **B** and **U** in the
536 same way as historical data. The method has applications in providing estimates of historical
537 land use and land-use change input data for modelling work in many domains, including
538 climate modelling (Lawrence *et al.*, 2016), ecosystem and biogeochemical modelling (Ogle *et*



539 *al.*, 2003; Ostle *et al.*, 2009), species distribution modelling (Martin *et al.*, 2013; Dainese *et*
540 *al.*, 2017), and socio-economics (Moran *et al.*, 2011; Sharmina *et al.*, 2016).

541 References

542 Alexander P, Prestele R, Verburg PH et al. (2017) Assessing uncertainties in land cover
543 projections. *Global Change Biology*, **23**, 767–781.

544 Azzalini A (2017) The R package sn: The Skew-Normal and Skew-t distributions (version
545 1.5-0). Università di Padova, Italia, pp.

546 Bradley R, Milne R, Bell J, Lilly A, Jordan C, Higgins A (2005) A soil carbon and land use
547 database for the United Kingdom. *Soil Use and Management*, **21**, 363–369.

548 Cannell MGR, Milne R, Hargreaves KJ et al. (1999) National Inventories of Terrestrial
549 Carbon Sources and Sinks: The U.K. Experience. *Climatic Change*, **42**, 505–530.

550 Dainese M, Isaac NJB, Powney GD et al. (2017) Landscape simplification weakens the
551 association between terrestrial producer and consumer diversity in Europe. *Global Change*
552 *Biology*, **23**, 3040–3051.

553 Dewar RC, Cannell MGR (1992) Carbon sequestration in the trees, products and soils of
554 forest plantations: An analysis using UK examples. *Tree Physiology*, **11**, 49–71.

555 Edwards P, Christie J (1981) Yield models for forest management. HMSO, London. HMSO,
556 London, 32 pp.

557 European Environment Agency (2016) Corine Land Cover 2012 raster data. *European*
558 *Environment Agency*.

559 Fisher JRB, Acosta EA, Dennedy-Frank PJ, Kroeger T, Boucher TM (2017) Impact of
560 satellite imagery spatial resolution on land use classification accuracy and modeled water



- 561 quality. *Remote Sensing in Ecology and Conservation*, n/a–n/a.
- 562 Fuchs R, Herold M, Verburg PH, Clevers JGPW (2013) A high-resolution and harmonized
563 model approach for reconstructing and analysing historic land changes in Europe. *Biogeo-*
564 *sciences*, **10**, 1543–1559.
- 565 Fuchs R, Schulp CJ, Hengeveld GM, Verburg PH, Clevers JG, Schelhaas M-J, Herold M
566 (2015) Assessing the influence of historic net and gross land changes on the carbon fluxes of
567 Europe. *Global Change Biology*, **22**, 2526–2539.
- 568 Fuller RM, Smith GM, Devereux BJ (2003) The characterisation and measurement of land
569 cover change through remote sensing: Problems in operational applications? *International*
570 *Journal of Applied Earth Observation and Geoinformation*, **4**, 243–253.
- 571 Gelman A, Rubin DB (1992) Inference from Iterative Simulation Using Multiple Sequences.
572 *Statistical Science*, **7**, 457–472.
- 573 Gelman A, Carlin JB, Stern HS, Dunson DB, Vehtari A, Rubin DB (2013) Bayesian Data
574 Analysis, Third Edition, 3 edition edn. Chapman and Hall/CRC, Boca Raton, 675 pp.
- 575 Geweke J (1992) Evaluating the Accuracy of Sampling-Based Approaches to the Calculation
576 of Posterior Moments. In: *In Bayesian Statistics*, pp. 169–193. University Press.
- 577 Gitz V, Ciais P (2003) Amplifying effects of land-use change on future atmospheric CO₂
578 levels. *Global Biogeochemical Cycles*, **17**, 1–1–1–9.
- 579 Griffin A, Bailey R, Brown P (2014) An Introduction to the UK's Greenhouse Gas Inventory.
580 Department of Energy & Climate Change, pp.
- 581 Hartig F, Minunno F, Paul S (2017) BayesianTools: General-Purpose MCMC and SMC
582 Samplers and Tools for Bayesian Statistics. pp.
- 583 Henrys PA, Bee EJ, Watkins JW, Smith NA, Griffiths RI (2015) Mapping natural capital:



- 584 Optimising the use of national scale datasets. *Ecography*, **38**, 632–638.
- 585 Hurtt GC, Frohling S, Fearon MG et al. (2006) The underpinnings of land-use history:
586 Three centuries of global gridded land-use transitions, wood-harvest activity, and resulting
587 secondary lands. *Global Change Biology*, **12**, 1208–1229.
- 588 Hurtt GC, Chini LP, Frohling S et al. (2011) Harmonization of land-use scenarios for the
589 period 1500–2100: 600 years of global gridded annual land-use transitions, wood harvest, and
590 resulting secondary lands. *Climatic Change*, **109**, 117–161.
- 591 Kato E, Kinoshita T, Ito A, Kawamiya M, Yamagata Y (2013) Evaluation of spatially
592 explicit emission scenario of land-use change and biomass burning using a process-based
593 biogeochemical model. *Journal of Land Use Science*, **8**, 104–122.
- 594 Krause A, Pugh TAM, Bayer AD, Lindeskog M, Arneth A (2016) Impacts of land-use history
595 on the recovery of ecosystems after agricultural abandonment. *Earth Syst. Dynam.*, **7**,
596 745–766.
- 597 Lawrence DM, Hurtt GC, Arneth A et al. (2016) The Land Use Model Intercomparison
598 Project (LUMIP) contribution to CMIP6: Rationale and experimental design. *Geosci. Model
599 Dev.*, **9**, 2973–2998.
- 600 Levy PE, Milne R (2004) Estimation of deforestation rates in Great Britain. *Forestry*, **77**,
601 9–16.
- 602 Levy PE, Friend AD, White A, Cannell MGR (2004) The influence of land use change on
603 global-scale fluxes of carbon from terrestrial ecosystems. *Climatic Change*, **67**, 185–209.
- 604 Lunt MF, Rigby M, Ganesan AL, Manning AJ (2016) Estimation of trace gas fluxes with
605 objectively determined basis functions using reversible-jump Markov chain Monte Carlo.
606 *Geosci. Model Dev.*, **9**, 3213–3229.
- 607 Martin Y, Van Dyck H, Dendoncker N, Titeux N (2013) Testing instead of assuming the



- 608 importance of land use change scenarios to model species distributions under climate change.
609 *Global Ecology and Biogeography*, **22**, 1204–1216.
- 610 Martin KL, Hwang T, Vose JM, Coulston JW, Wear DN, Miles B, Band LE (2017) Water-
611 shed impacts of climate and land use changes depend on magnitude and land use context.
612 *Ecohydrology*, n/a–n/a.
- 613 Milne R, Brown TA (1997) Carbon in the Vegetation and Soils of Great Britain. *Journal of*
614 *Environmental Management*, **49**, 413–433.
- 615 Moran D, Macleod M, Wall E et al. (2011) Marginal Abatement Cost Curves for UK
616 Agricultural Greenhouse Gas Emissions. *Journal of Agricultural Economics*, **62**, 93–118.
- 617 Newbold T, Hudson LN, Hill SLL et al. (2015) Global effects of land use on local terrestrial
618 biodiversity. *Nature*, **520**, 45–50.
- 619 Norton LR, Maskell LC, Smart SS et al. (2012) Measuring stock and change in the GB
620 countryside for policy – Key findings and developments from the Countryside Survey 2007
621 field survey. *Journal of Environmental Management*, **113**, 117–127.
- 622 Ogle SM, Jay Breidt F, Eve MD, Paustian K (2003) Uncertainty in estimating land use and
623 management impacts on soil organic carbon storage for US agricultural lands between 1982
624 and 1997. *Global Change Biology*, **9**, 1521–1542.
- 625 Ostle N, Levy P, Evans C, Smith P (2009) UK land use and soil carbon sequestration. *Land*
626 *Use Policy*, **26**, S274–S283.
- 627 Penman J, Gytarsky M, Hiraishi T et al. (2003) Good Practice Guidance for Land Use,
628 Land-Use Change and Forestry. Intergovernmental Panel on Climate Change, 632 pp.
- 629 Phelps LN, Kaplan JO (2017) Land use for animal production in global change studies:
630 Defining and characterizing a framework. *Global Change Biology*, n/a–n/a.
- 631 Piano E, De Wolf K, Bona F et al. (2017) Urbanization drives community shifts towards



632 thermophilic and dispersive species at local and landscape scales. *Global Change Biology*, **23**,
633 2554–2564.

634 Post WM, Kwon KC (2000) Soil carbon sequestration and land-use change: Processes and
635 potential. *Global change biology*, **6**, 317–327.

636 Prestele R, Arneth A, Bondeau A et al. (2017) Current challenges of implementing anthro-
637 pogenic land-use and land-cover change in models contributing to climate change assessments.
638 *Earth Syst. Dynam.*, **8**, 369–386.

639 Quesada B, Arneth A, de Noblet-Ducoudré N (2017) Atmospheric, radiative, and hydrologic
640 effects of future land use and land cover changes: A global and multimodel climate picture.
641 *Journal of Geophysical Research: Atmospheres*, **122**, 2016JD025448.

642 Raftery AE, Lewis SM (1992) Comment: One Long Run with Diagnostics: Implementation
643 Strategies for Markov Chain Monte Carlo. *Statistical Science*, **7**, 493–497.

644 Reich S (2015) Probabilistic Forecasting and Bayesian Data Assimilation, Reprint edition
645 edn. Cambridge University Press, Cambridge, 308 pp.

646 Rounsevell M, Reginster I, Araújo M et al. (2006) A coherent set of future land use change
647 scenarios for Europe. *Agriculture, Ecosystems & Environment*, **114**, 57–68.

648 Rowland C, Morton R, Carrasco L, McShane G, O’Neil A, Wood C (2017) Land Cover Map
649 2015 (25m raster, GB).

650 Scott WA (2008) Countryside Survey. Statistical Report. Centre For Ecology and Hydrology,
651 Lancaster, pp.

652 Scottish Government SAH (2017) Agriculture and Fisheries - Publications.

653 Sharmina M, Hoolohan C, Bows-Larkin A et al. (2016) A nexus perspective on competing
654 land demands: Wider lessons from a UK policy case study. *Environmental Science & Policy*,



655 **59**, 74–84.

656 Tomlinson S, Ulrike Dragosits, Peter E. Levy, Amanda M. Thomson, Janet Moxley (2017)
657 Quantifying gross vs. net agricultural land use change in Great Britain using the Integrated
658 Administration and Control System. *Science of The Total Environment*, **submitted**.

659 Van Oijen M (2017) Bayesian Methods for Quantifying and Reducing Uncertainty and Error
660 in Forest Models. *Current Forestry Reports*.

661 Wikle CK, Berliner LM (2007) A Bayesian tutorial for data assimilation. *Physica D: Nonlinear*
662 *Phenomena*, **230**, 1–16.

663 Wilkenskjeld S, Kloster S, Pongratz J, Raddatz T, Reick CH (2014) Comparing the influence
664 of net and gross anthropogenic land-use and land-cover changes on the carbon cycle in the
665 MPI-ESM. *Biogeosciences*, **11**, 4817–4828.

666 Wood CM, Smart SM, Bunce RGH et al. (2017) Long-term vegetation monitoring in Great
667 Britain – the Countryside Survey 1978–2007 and beyond. *Earth System Science Data*, **9**,
668 445–459.